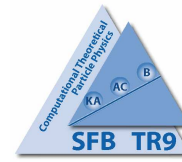


QCD Analysis of the Polarized DIS World Data

Johannes Blümlein and Helmut Böttcher



- Data
- The NLO Analysis and Fit Results
- Polarized PDFs
- Λ_{QCD} and $\alpha_s(M_Z^2)$
- Higher Twist Contributions
- Conclusions

Nucl.Phys.B841:205-230,2010

The Data

| Experiment | x -range | Q^2 -range [GeV ²] | data points | | \mathcal{N}_i |
|------------|---------------|-------------------------------------|-------------|------|-----------------|
| | | | type | # | |
| E143(p) | 0.027 – 0.749 | 1.17 – 9.52 | g_1/F_1 | 82 | 0.963 |
| HERMES(p) | 0.026 – 0.731 | 1.12 – 14.29 | A_1 | 37 | 0.970 |
| E155(p) | 0.015 – 0.750 | 1.22 – 34.72 | g_1/F_1 | 24 | 1.003 |
| SMC(p) | 0.004 – 0.484 | 1.14 – 72.10 | A_1 | 59 | 0.960 |
| EMC(p) | 0.015 – 0.466 | 3.50 – 29.5 | A_1 | 10 | 0.964 |
| CLAS1(p) | 0.125 – 0.575 | 1.10 – 4.16 | A_1 | 10 | 1.010 |
| CLAS2(p) | 0.292 – 0.592 | 1.01 – 4.96 | g_1/F_1 | 191 | 1.030 |
| COMPASS(p) | 0.005 – 0.568 | 1.10 – 62.10 | A_1 | 15 | 0.955 |
| proton | | | | 428 | |
| E143(d) | 0.027 – 0.749 | 1.17 – 9.52 | g_1/F_1 | 82 | 0.960 |
| HERMES(d) | 0.026 – 0.731 | 1.12 – 14.29 | A_1 | 37 | 0.970 |
| E155(d) | 0.015 – 0.750 | 1.22 – 34.79 | g_1/F_1 | 24 | 0.979 |
| SMC(d) | 0.004 – 0.483 | 1.14 – 71.76 | A_1 | 65 | 0.998 |
| COMPASS(d) | 0.005 – 0.566 | 1.10 – 55.30 | A_1 | 15 | 0.952 |
| CLAS1(d) | 0.125 – 0.575 | 1.01 – 4.16 | A_1 | 10 | 1.003 |
| CLAS2(d) | 0.298 – 0.636 | 1.01 – 4.16 | g_1/F_1 | 662 | 1.014 |
| deuteron | | | | 895 | |
| E142(n) | 0.035 – 0.466 | 1.10 – 5.50 | A_1 | 33 | 0.989 |
| HERMES(n) | 0.033 – 0.464 | 1.22 – 5.25 | g_1 | 9 | 0.970 |
| E154(n) | 0.017 – 0.564 | 1.20 – 15.00 | g_1 | 17 | 0.980 |
| JLAB(n) | 0.330 – 0.600 | 2.71 – 4.83 | g_1 | 3 | 1.000 |
| neutron | | | | 62 | |
| total | | | | 1385 | |

Table 1: Number of data points on A_1 , g_1/F_1 or g_1 for $Q^2 > 1.0 \text{ GeV}^2$ and $W^2 > 3.24 \text{ GeV}^2$ used in the present QCD analysis. For each experiment are given the x and Q^2 ranges, the type of quantity measured, the number of data points for each given target, and the fitted normalization shifts \mathcal{N}_i (see text).

Evolution Equations

$$\left[M \frac{\partial}{\partial M} + \beta(g) \frac{\partial}{\partial g} - 2\gamma_\psi(g) \right] F_i(N) = 0$$

$$\left[M \frac{\partial}{\partial M} + \beta(g) \frac{\partial}{\partial g} + \gamma_\kappa^N(g) - 2\gamma_\psi(g) \right] f_k(N) = 0$$

$$\left[M \frac{\partial}{\partial M} + \beta(g) \frac{\partial}{\partial g} - \gamma_\kappa^N(g) \right] C_j^k(N) = 0$$

CALLAN–SYMNANZIK equations for mass factorization

≡ ALTARELLI–PARISI evolution equations

x-space :

$$\frac{d}{d \log(\mu^2)} \begin{pmatrix} q^+(x, Q^2) \\ G(x, Q^2) \end{pmatrix} = \frac{\alpha_s}{2\pi} \mathbf{P}(x, \alpha_s) \otimes \begin{pmatrix} q^+(x, Q^2) \\ G(x, Q^2) \end{pmatrix}$$

$$\mathbf{P}(x, \alpha_s) = \mathbf{P}^{(0)}(x) + \frac{\alpha_s}{2\pi} \mathbf{P}^{(1)}(x) + \left(\frac{\alpha_s}{2\pi} \right)^2 \mathbf{P}^{(2)}(x) + \dots$$

The NLO Fit Results

| | | | | | |
|--|----------|-------------------|---------------------------------|----------|----------------------------|
| Δu_v | η | 0.928 (fixed) | $\Delta \bar{q}_s$ | η | -0.417 ± 0.079 |
| | a | 0.239 ± 0.027 | | a | 0.365 ± 0.164 |
| | b | 3.031 ± 0.178 | | b | 8.080 (fixed) |
| | ρ | 0.0 (fixed) | | ρ | 0.0 (fixed) |
| | γ | 27.64 (fixed) | | γ | 0.0 (fixed) |
| Δd_v | η | -0.342 (fixed) | ΔG | η | 0.461 ± 0.430 |
| | a | 0.128 ± 0.068 | | a | $a_{\Delta \bar{q}_s} + 1$ |
| | b | 4.055 ± 0.879 | | b | 5.610 (fixed) |
| | ρ | 0.0 (fixed) | | ρ | 0.0 (fixed) |
| | γ | 44.26 (fixed) | | γ | 0.0 (fixed) |
| $\Lambda_{QCD}^{(4)} = 243 \pm 62 \text{ MeV}$ | | | $\chi^2/NDF = 1537/1377 = 1.12$ | | |

Table 2: Final parameter values and their statistical errors at the input scale $Q_0^2 = 4.0 \text{ GeV}^2$.

The Correlation Matrix

| | $\Lambda_{QCD}^{(4)}$ | a_{u_v} | b_{u_v} | a_{d_v} | b_{d_v} | η_{sea} | a_{sea} | η_G |
|-----------------------|-----------------------|----------------|----------------|----------------|----------------|----------------|----------------|----------------|
| $\Lambda_{QCD}^{(4)}$ | 3.85E-3 | | | | | | | |
| a_{u_v} | -4.08E-4 | 7.55E-4 | | | | | | |
| b_{u_v} | -1.14E-3 | 4.30E-3 | 3.18E-2 | | | | | |
| a_{d_v} | 2.75E-3 | -9.39E-4 | -4.44E-3 | 4.61E-3 | | | | |
| b_{d_v} | 2.38E-2 | -8.34E-3 | -1.03E-2 | 4.51E-2 | 7.73E-1 | | | |
| η_{sea} | 1.79E-3 | -7.20E-4 | -3.79E-3 | 2.38E-3 | 2.23E-2 | 6.32E-3 | | |
| a_{sea} | -5.65E-3 | 3.04E-3 | 1.65E-2 | -8.26E-3 | -7.39E-2 | 8.07E-4 | 2.70E-2 | |
| η_G | -1.96E-2 | 8.32E-3 | 4.25E-2 | -2.16E-2 | -1.68E-1 | -2.21E-2 | 4.17E-2 | 1.85E-1 |

Table 3: The covariance matrix for the 7 + 1 parameter NLO fit based on the world asymmetry data.

The Polarized PDFs @ $Q^2 = 4 \text{ GeV}^2$

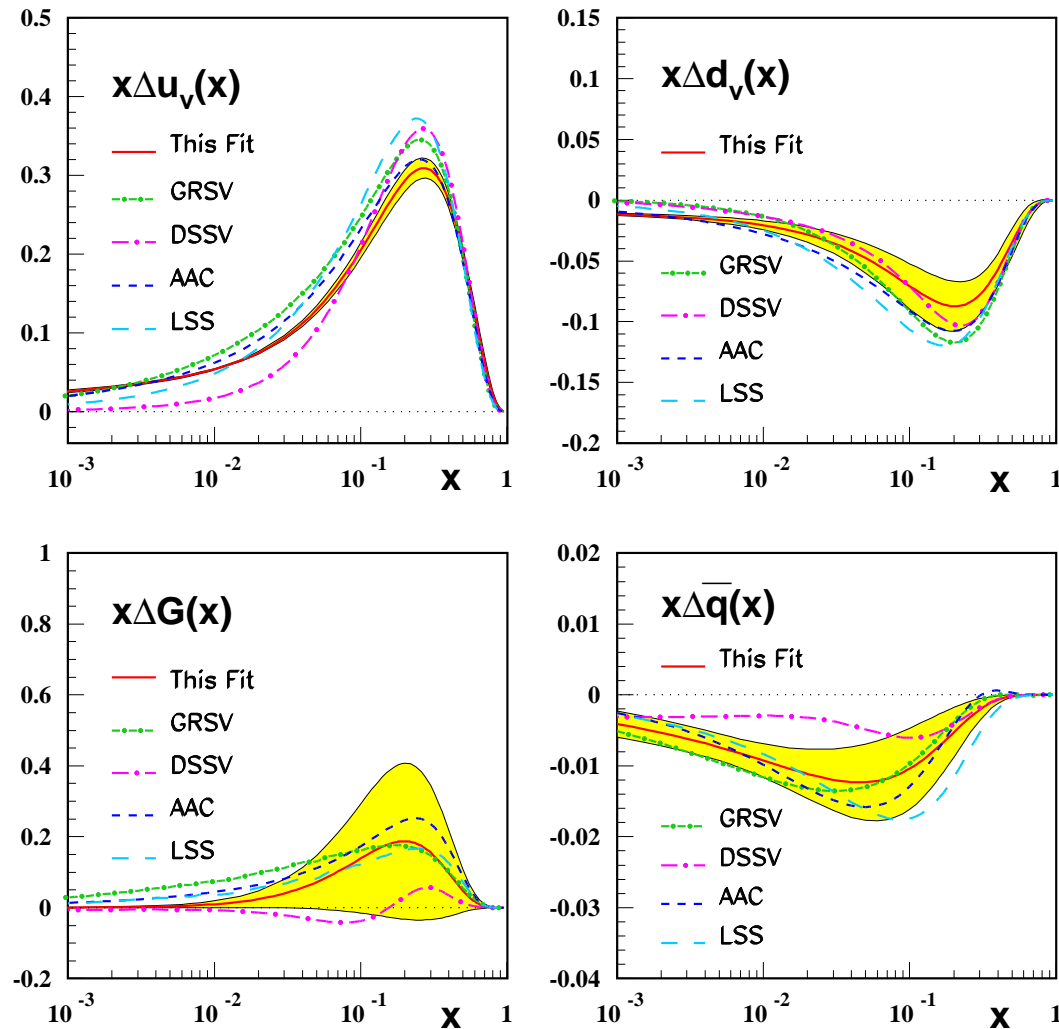


Figure 1: NLO polarized parton distributions at the input scale $Q_0^2 = 4.0 \text{ GeV}^2$ (solid line) compared to results obtained by GRSV (dashed-dotted line), DSSV (long dashed-dotted line), AAC (dashed line), and LSS (long dashed line). The shaded areas represent the fully correlated 1σ error bands calculated by Gaussian error propagation.

The Gluon Distribution

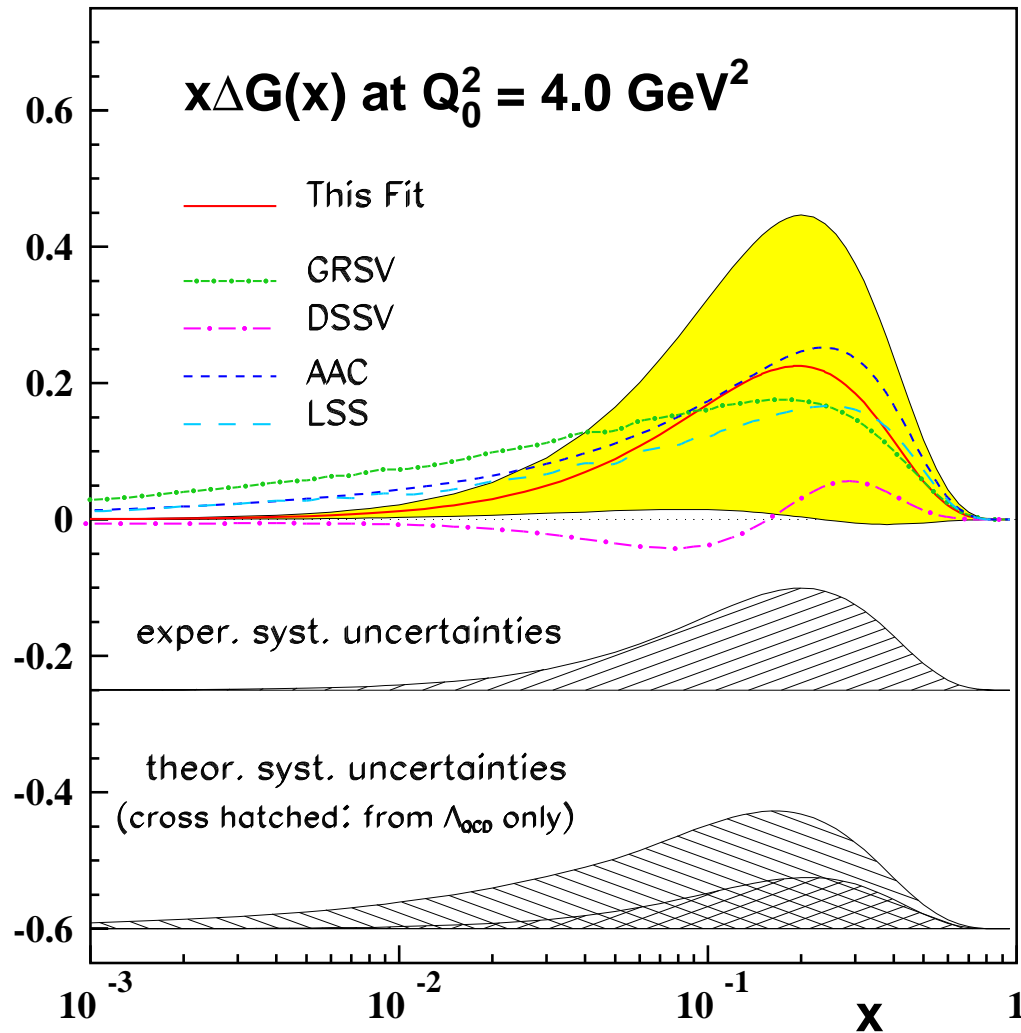


Figure 2: The polarized parton density $x\Delta G(x)$ at $Q_0^2 = 4.0 \text{ GeV}^2$ as function of x (solid line). The shaded area is the fully correlated 1σ statistical error band and the hatched areas are the systematic uncertainties. Results from GRSV (dashed-dotted line), DSSV (long dashed-dotted line), AAC (dashed line), and LSS (long dashed line) are shown for comparison.

The Singlet Distribution

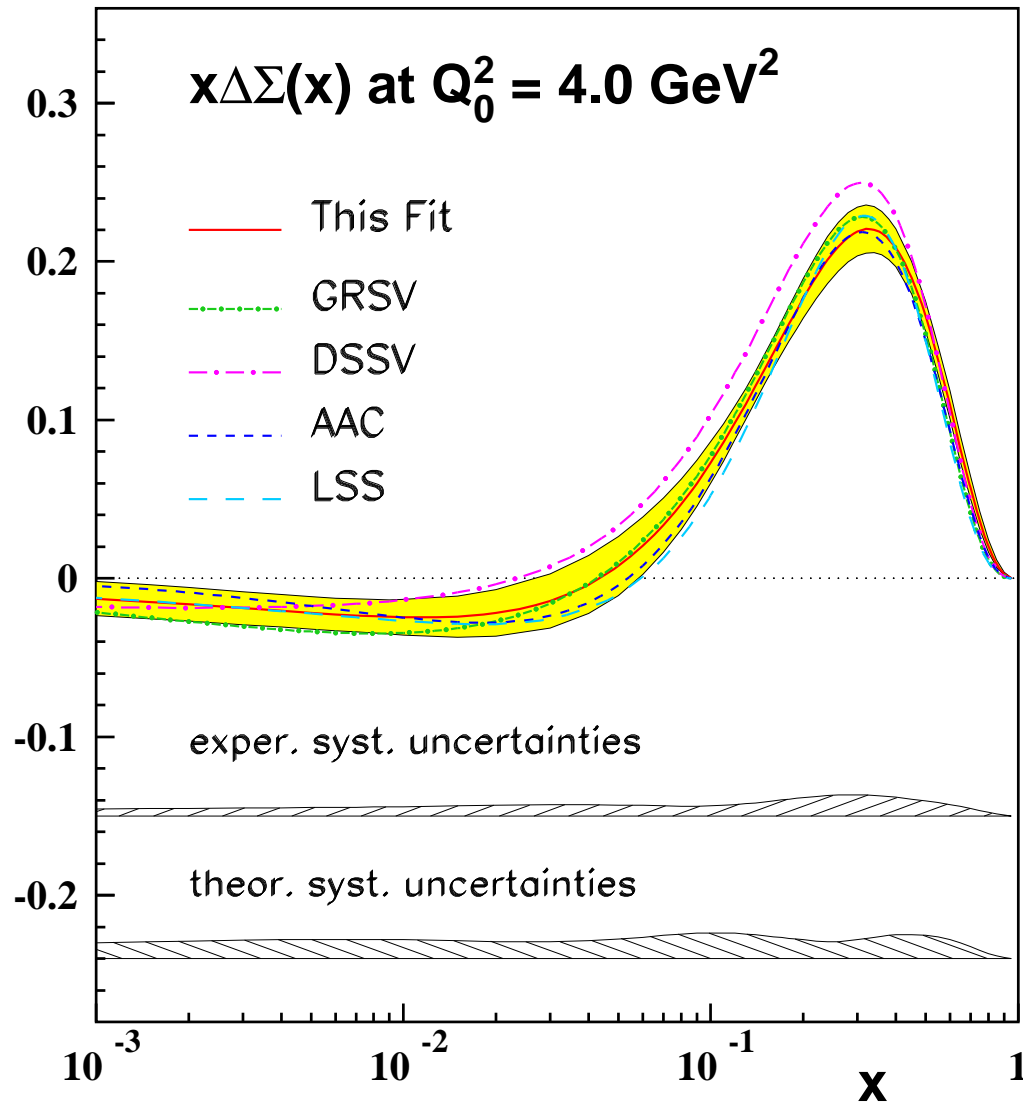


Figure 3: The polarized parton density $x\Delta\Sigma(x)$ at $Q_0^2 = 4.0 \text{ GeV}^2$ as function of x (solid line). The shaded area is the fully correlated 1σ statistical error band and the hatched areas are the systematic uncertainties. Results from GRSV (dashed-dotted line), DSSV (long dashed-dotted line), AAC (dashed line), and LSS (long dashed line) are shown for comparison.

The Fit and the Data

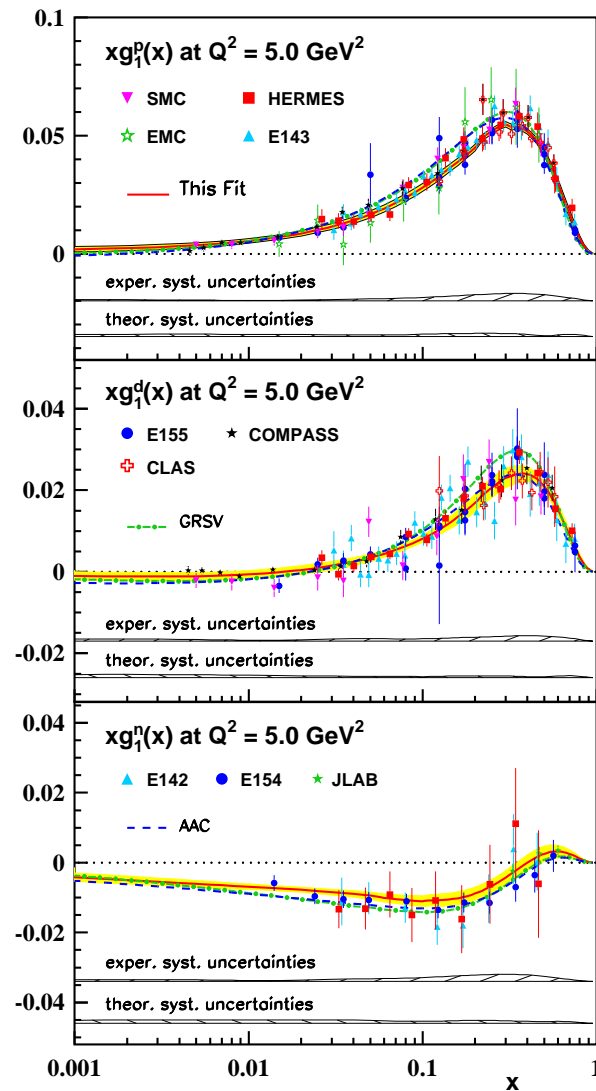


Figure 4: The spin-dependent structure functions $xg_1^p(x)$, $xg_1^d(x)$ and $xg_1^n(x)$ as function of x . The experimental data are evolved to a common value of $Q^2 = 5 \text{ GeV}^2$. The error bars shown are the statistical and systematic ones added in quadrature. The experimental distributions are well described (solid curve) within the statistical (shaded areas) and systematic (hatched areas) error bands. Shown for comparison are the curves obtained by GRSV (dashed-dotted) and AAC (dashed).

The Fit and the Data

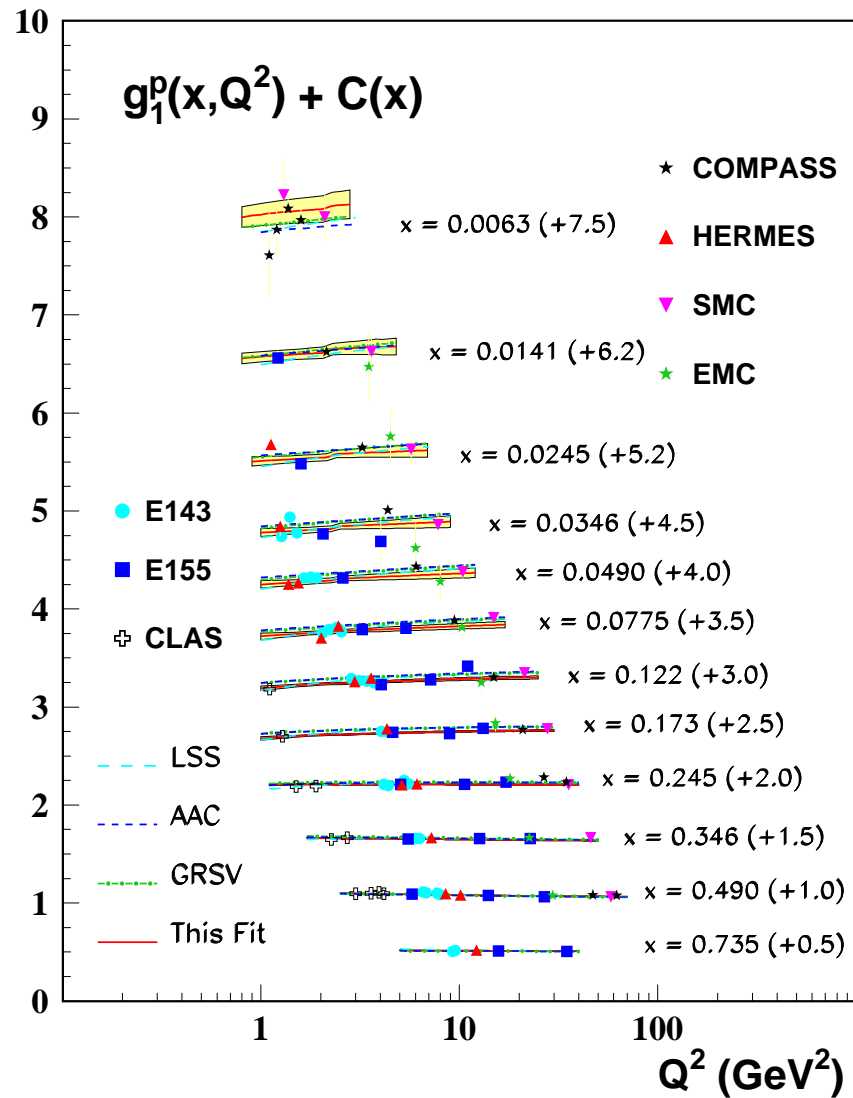


Figure 5: The spin-dependent structure functions $xg_1^p(x)$, $xg_1^d(x)$ and $xg_1^n(x)$ as function of x . The experimental data are evolved to a common value of $Q^2 = 5 \text{ GeV}^2$. The error bars shown are the statistical and systematic ones added in quadrature. The experimental distributions are well described (solid curve) within the statistical (shaded areas) and systematic (hatched areas) error bands. Shown for comparison are the curves obtained by GRSV (dashed-dotted) and AAC (dashed).

$$\alpha_s(M_Z^2)$$

S. Alekhin, J.B., S. Klein, S. Moch, Phys.Rev.D81 (2010) 014032

$$\frac{\delta\alpha_s(M_Z^2)}{\alpha_s(M_Z^2)} \approx 1.2\%$$

| | $\alpha_s(M_Z^2)$ | |
|----------------|--------------------------------|--------------------------------------|
| ABKM | 0.1135 ± 0.0014 | HQ: FFS $N_f = 3$ |
| A.Hoang et al. | $0.1135 \pm 0.0011 \pm 0.0006$ | e^+e^- thrust |
| ABKM | 0.1129 ± 0.0014 | HQ: BSMN-approach |
| BBG (2006) | $0.1134^{+0.0019}_{-0.0021}$ | valence analysis, NNLO |
| JR (2008) | 0.1124 ± 0.0020 | dynamical approach |
| MSTW (2008) | 0.1171 ± 0.0014 | |
| H1/ZEUS (2010) | 0.1145 ± 0.0042 | (combined H1/ZEUS data, preliminary) |
| ABM (2010) | 0.1147 ± 0.0012 | (FFN, combined H1/ZEUS data in) |
| BBG (2006) | $0.1141^{+0.0020}_{-0.0022}$ | valence analysis, N ³ LO |
| WA (2009) | 0.1184 ± 0.0007 | |

$\alpha_s(M_Z^2)$ and $\Lambda_{\text{QCD}}^{(4)}$

$$\Lambda_{\text{QCD}}^{(4)} = 243.5 \pm 62 \text{ (exp)} \quad \begin{matrix} -37 \\ +21 \end{matrix} \text{ (FS)} \quad \begin{matrix} +46 \\ -87 \end{matrix} \text{ (RS)}.$$

$$\alpha_s(M_Z^2) = 0.1132 \quad \begin{matrix} +0.0043 \\ -0.0051 \end{matrix} \text{ (exp)} \quad \begin{matrix} -0.0029 \\ +0.0015 \end{matrix} \text{ (FS)} \quad \begin{matrix} +0.0032 \\ -0.0075 \end{matrix} \text{ (RS)} .$$

Earlier values :

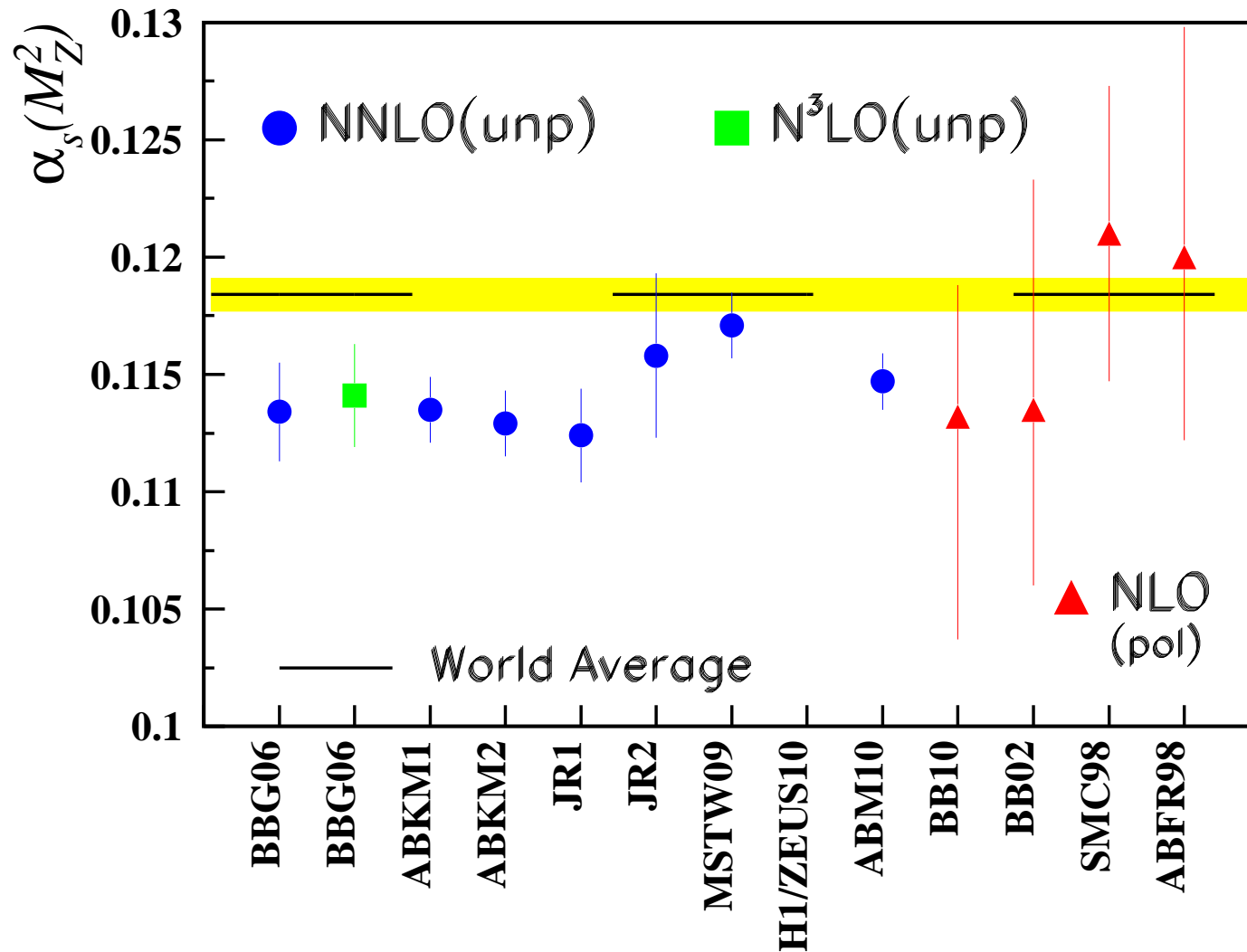
$$\text{E154 :} \quad \alpha_s(M_Z^2) = 0.108 - 0.116$$

$$\text{SMC :} \quad \alpha_s(M_Z^2) = 0.121 \pm 0.007$$

$$\text{ABFR :} \quad \alpha_s(M_Z^2) = 0.120 \quad \begin{matrix} +0.100 \\ -0.008 \end{matrix}$$

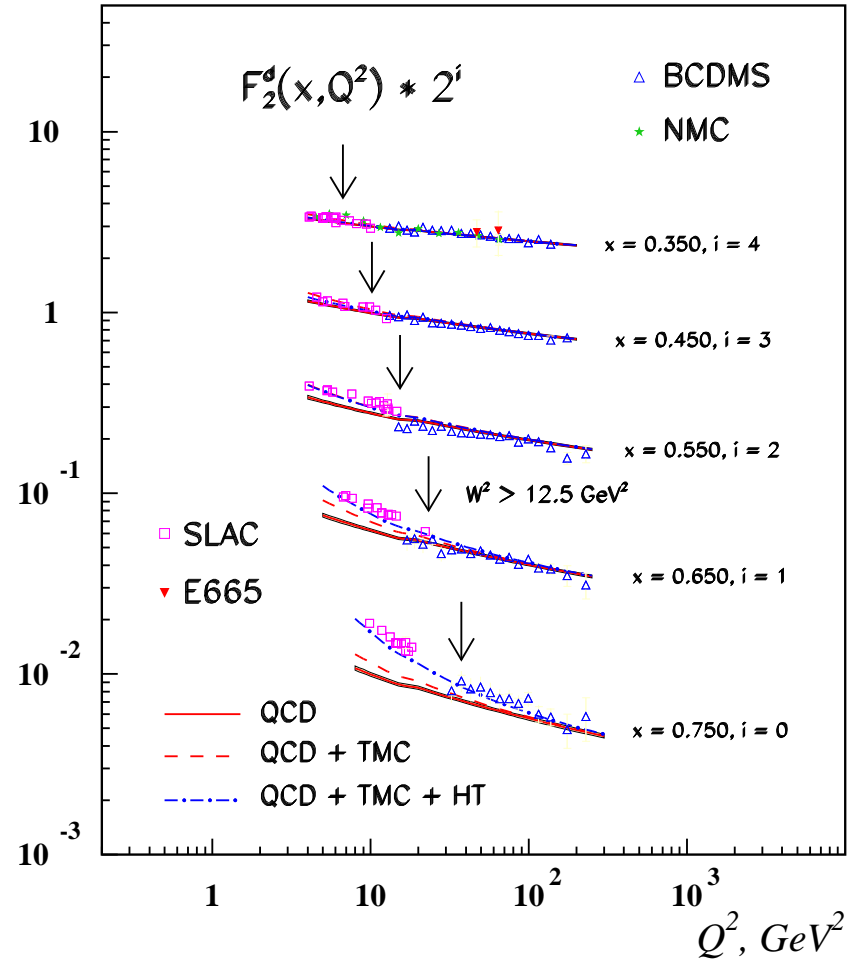
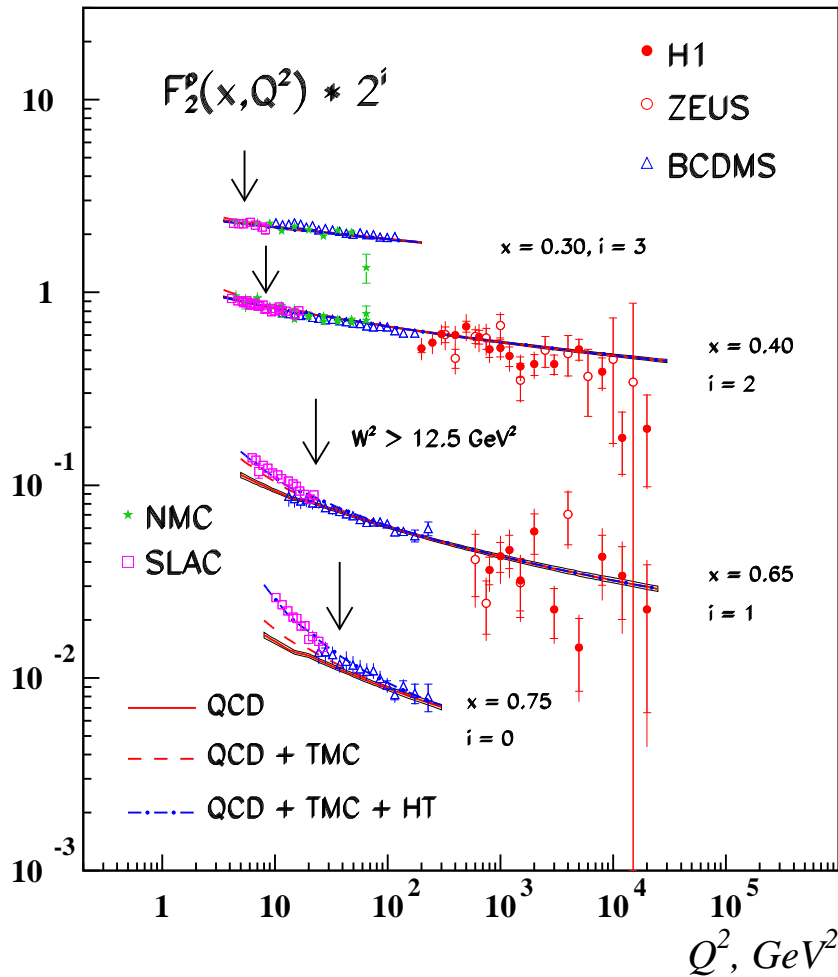
$$\text{BB02 :} \quad \alpha_s(M_Z^2) = 0.114 \quad \begin{matrix} +0.100 \\ -0.008 \end{matrix}$$

$$\alpha_s(M_Z^2)$$

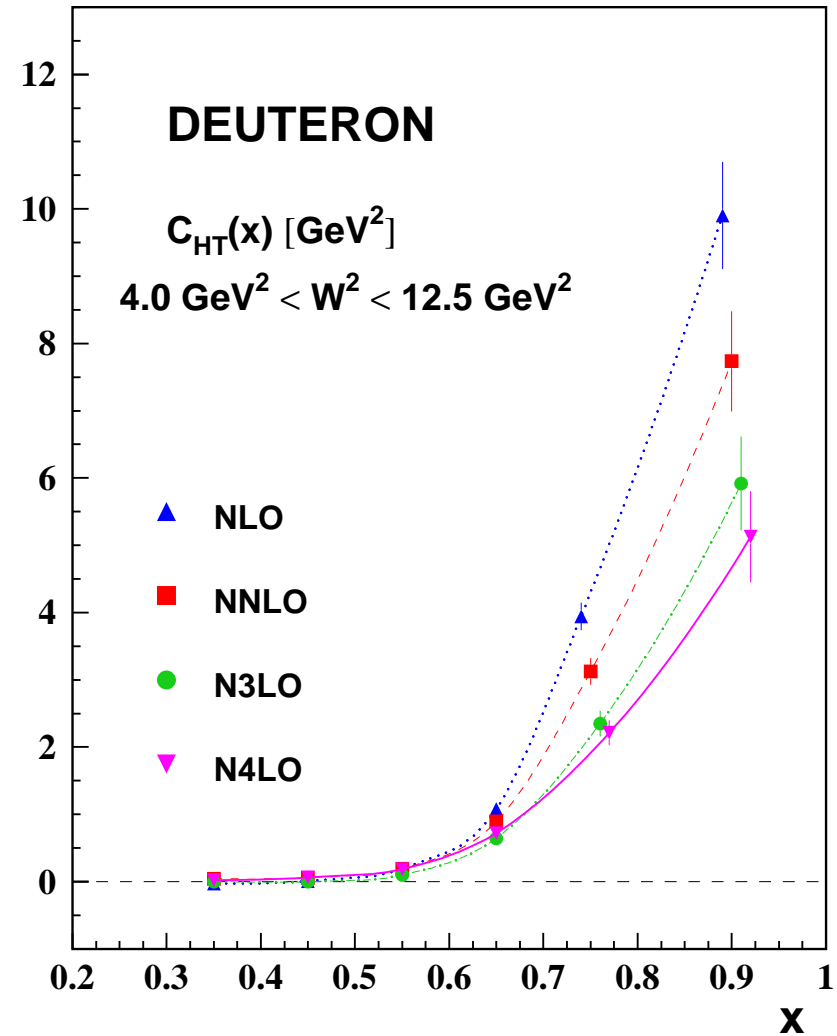
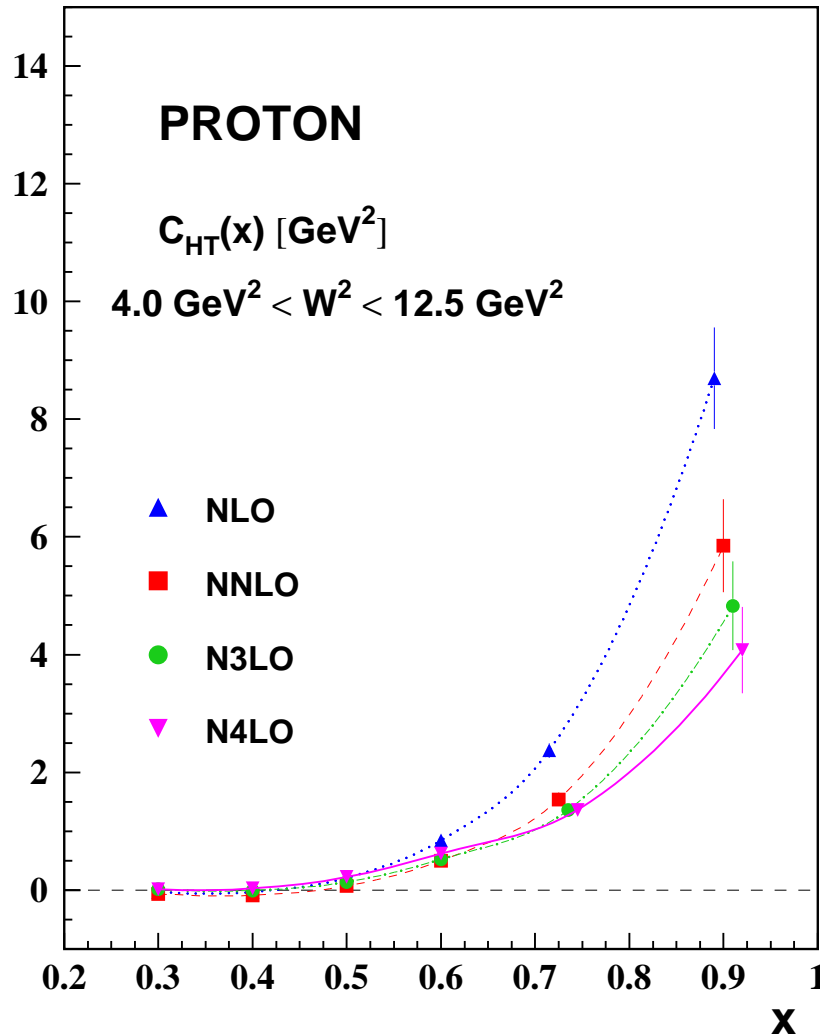


World average: S. Bethke, Eur.Phys.J.C64:689-703,2009; yellow band.

Valence Distributions

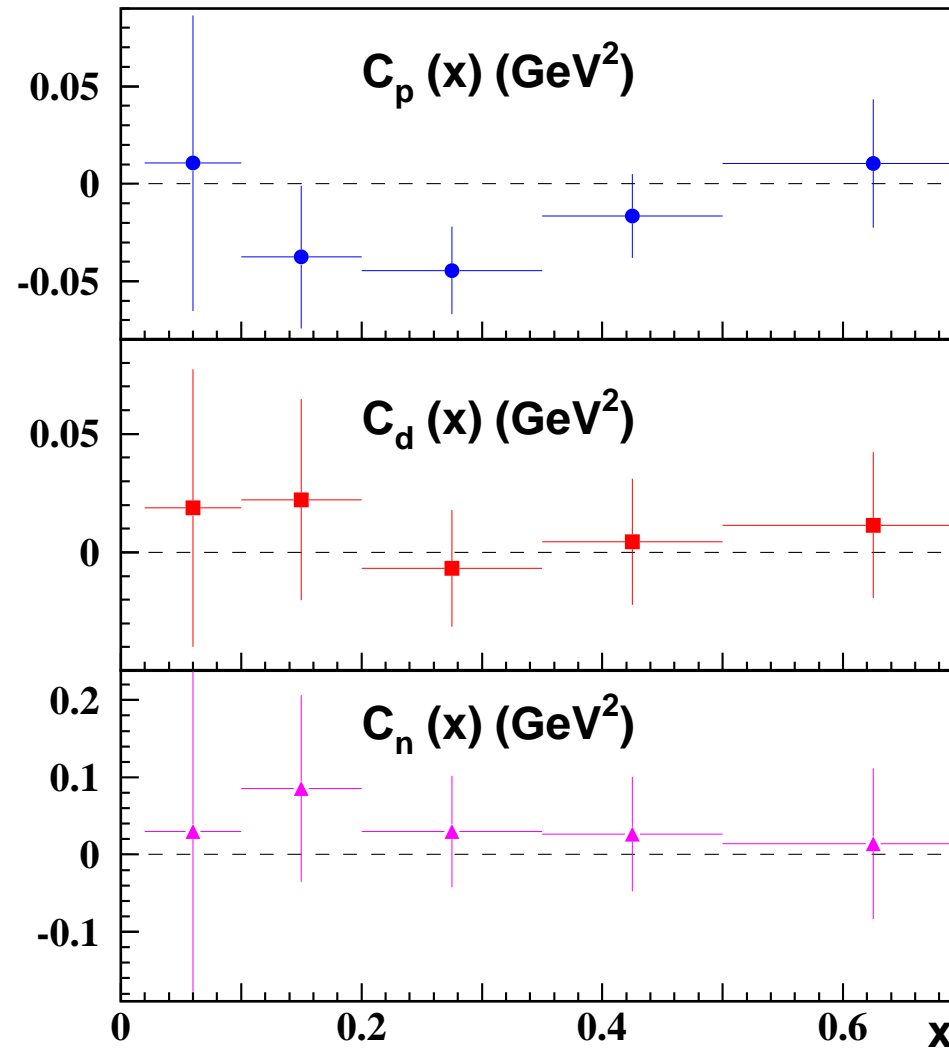


Valence Distributions: higher twist



- agreement between p and d analysis, J.B., H. Böttcher, 2008
- LGT determination of interest

Higher Twist



$$g_1(x, Q^2) = g_1^{\text{LT}}(x, Q^2) + \frac{C_{\text{HT}}(x)}{Q^2}$$

Higher Twist

| $\langle x \rangle$ | $C_p[\text{GeV}^2]$ | $C_d[\text{GeV}^2]$ | $C_p[\text{GeV}^2]$ | $C_d[\text{GeV}^2]$ |
|---------------------|---------------------|---------------------|---------------------|---------------------|
| | multiplicative | | additive | |
| 0.060 | -0.084 ± 0.245 | 0.007 ± 0.287 | 0.011 ± 0.076 | 0.019 ± 0.059 |
| 0.150 | -0.229 ± 0.156 | 0.169 ± 0.431 | -0.038 ± 0.037 | 0.022 ± 0.042 |
| 0.275 | -0.224 ± 0.099 | -0.226 ± 0.270 | -0.045 ± 0.022 | -0.007 ± 0.025 |
| 0.425 | -0.083 ± 0.140 | -0.013 ± 0.384 | -0.017 ± 0.021 | 0.005 ± 0.027 |
| 0.625 | 0.290 ± 0.417 | 0.061 ± 1.106 | 0.011 ± 0.033 | 0.011 ± 0.031 |

Table 5: The higher twist coefficients $C_p(x)$ and $C_d(x)$ as function of x .

Conclusions

- An NLO analysis of the current polarized DIS World data has been performed accounting for all parameter correlations.
- Grids including correlated errors of the parameterization are provided.
- The gluon density comes out lower than in previous analyses.
- $\Lambda_{\text{QCD}}^{(4)}$ and $\alpha_s(M_Z^2)$ have been measured. Similar central values as in the BB02 analysis and recent N²⁽³⁾LO DIS unpolarized world data analyses are obtained. The NLO FS/RS variations still imply a large uncertainty at NLO if compared to the experimental error.
- We determined the higher twist contributions which are found to be compatible with zero within the present errors both for proton and deuteron targets.
- NLO Moments with correlated errors can be provided for comparisons with LGT simulations.